Electronic Supplementary Information (ESI)

Unravelling the role of various interactions in mechanochromism induced polymorphism: acid fumes sensor kit and double encryption decryption technologies

*Pranjalee Yadav, Aayoosh Singh, Amit Kumar Singh and Vinod P. Singh**

Email: singhvp@bhu.ac.in, singvp@yahoo.co.in

Table of Contents

1. EXPERIMENTAL SECTION

1.1. Reagents

Except where noted, all the chemicals and reagents were acquired from commercial sources and used without further purification. Pyrene-1-carbaldehyde and furan-2-carbohydrazide were procured from Sigma-Aldrich Chemicals, USA. Methanol, absolute ethanol and DMF obtained from Merck, India and were used after being checking its purity using UV-visible and photoluminescence spectral methods. All of the experiments were performed using Millipore water.

1.2. Physical measurements

FT-IR spectrum was collected using KBr pellet method in the 4000-400 cm^{-1} region on a FT-IR 4700 JASCO spectrophotometer. ^{1}H and ^{13}C-NMR spectra in DMSO-d_6 were obtained using JEOL Resonance Inc (Model-ECZ-500R) multinuclear FT-NMR spectrometer. Coupling constants in hertz (Hz), while chemical shifts are reported in parts per million (ppm) with regard to an internal standard of tetramethylsilane (TMS). HRMS SCIEX X-500R QTOF spectrometer has been utilized to collect mass spectrum at room temperature. UV-visible spectra were collect using Shimadzu UV-1800 spectrophotometer. Fluromax 4CP plus Fluorescence Spectrophotometer (slit width = 2 nm) has been used for obtaining all the photoluminescence spectra. Witec Alpha 300 RAS (made in Germany) with a 405 nm pulsed diode laser was used to record TRPL. Malvern Panalytical (UK). A Bruker D 8 Advance powder X-ray diffractometer equipped with Cu Kα radiation with a LyneEye detector was used for the powder X-ray diffraction experiments. Solid state photoluminescence was recorded on a Fluorolog FL-3C-21 UV-Vis-NIR-Spectrofluorometer with an integrated sphere (steady-state). Thermal property was analysed by differential scanning calorimetry (DSC) on a Mettler Toledo Model-822e instrument in nitrogen environment at the heating rate of 10 ^{o}C/min.

1.3. SEM analysis

The EVO-Scanning Electron Microscope MA15/18 was used to capture the SEM images. SEM measurements for PCFH (20 μM) at various fraction of THF/H_2O (f_w: 80 % and 99 %) were carried out by drop casting on cover slip and coating it with silver.

1.4. DLS analysis

DLS measurements for PCFH at various fraction of THF/H_2O (f_w: 80 % and 99 %) were conducted on a Zetasizer Ultra (ZSU5700) Malvern Panalytical (UK) Particle Size Analyzer.

1.5. X-ray Crystallography

The Rigaku XtaLAB Synergy-I diffractometer with CrysAlisPro was used to conduct the single crystal X-ray diffraction studies, with a graphite monochromated Cu Kα (λ = 1.54184) radiation source. At ambient temperature, measurements were taken of the probe and metal complex. The structure was solved with SHELXL-97 and optimized with full matrix least-squares on F2 and anisotropic displacement parameters for all non-hydrogen atoms.[44,45] All hydrogen atoms were refined into their geometrically ideal positions using riding model. The structure was generated using the MERCURY program and the ORTEP-3 Windows application.[46] The crystallographic data and structure determination information has been tabulated in Table S3 and S4. CCDC **2356829** and **2493464** include the crystallographic data of PCFH-P and PCFH-G, respectively.

1.6. Computational details

Density functional theory has been performed using Gaussian-09 program for geometry optimization. B3LYP exchange-correlation functional with basis set 6-311++g(d, p) has been used to theoretically optimize the lowest energy spatial conformations of PCFH and protonated PCFH.[47]

1.7. Hirshfeld Surface Analysis

Hirshfeld surface analysis has been carried out to demonstrate various intermolecular interactions in two polymorphs namely PCFH-P and PCFH-G. Two-dimensional fingerprint plots were produced using *CrystalExplorer3* program. The structural input files were obtained in the CIF format. Hirshfeld surface was represented by d_i and d_e, denoting the distance from the nearest atom inside and outside of the surface, respectively. Both d_i and d_e, were used to designate the normalized contact distance (d_{norm}).

1.8. Fluorescence quantum yield measurements

Fluorescence quantum yield was determined from the following equation:[48]

$$\Phi = \Phi_r\left(\frac{I}{I_r}\right)\left(\frac{ODr}{OD}\right)\left(\frac{n^2}{n_r^2}\right)$$

Here, ***I*** refer to integrated fluorescence intensity, ***Φ*** refers to fluorescence quantum yield, ***n*** refers to refractive index of solvents and ***OD*** is the absorption (optical density). The subscript ***r*** is used for reference. Herein, Φ_r signifies the quantum yield of reference quinine sulphate in 0.1 M H_2SO_4 (i.e., 0.54).

1.9. Fluorescence decay measurements

Time-resolved fluorescence lifetime experiments of PCFH (20 μM) for AIE studies have been recorded using a time-correlated single photon counting (TCSPC) system from Horiba Yovin (Delta Flex). Compounds were excited at 520 nm using a pico-second diode laser (Model:delta diode). Data analysis has been performed using decay analysis software (HORIBA Scientific: EzTime).

The dynamic parameters and weighted mean lifetime <τ> were computed using the following equations:

$$y = A_1 * \exp\left(-\frac{x}{\tau_1}\right) + A_2 * exp\left(-\frac{x}{\tau_2}\right) + y_0$$

$$<\tau> = \frac{A_1\tau_1 + A_2\tau_2}{A_1 + A_2}$$

Where, τ_1/τ_2 and A_1/A_2 are the lifetimes (τ) and fractions or amplitudes (A), respectively.

The following equations are used to calculate the radiative rate constant (K_r) and non-radiative rate constant (K_{nr}):[49]

$$<\tau^{-1}> = (K_r + K_{nr})$$

$$K_r = \frac{\Phi}{<\tau>}$$

2. Synthesis and characterization of *(E)-N'*-(anthracen-9-ylmethylene)furan-2-carbohydrazide (PCFH)

Ethanolic solutions of Pyrene-1-carbaldehyde (2.30 g, 10 mmol) and furan-2-carbohydrazide (1.26 g, 10 mmol) were mixed in round bottom flask. The reaction mixture was refluxed for 4 h on magnetic stirrer. The progress of reaction was monitored with thin-layer chromatography (TLC). The resulting light-yellow solid product was then filtered, washed

with ethanol and dried over anhydrous $CaCl_2$ (Scheme 1). Yield 85 %. M.P. 250 °C, *Anal. Calc.* for $C_{22}H_{14}N_2O_2$ (338): HRMS *m/z:* 339.1134 $[M+H]^+$, 361.0951$[M+Na]^+$. IR (cm^{-1}): ν(N-H) 3224, ν(Ar C-H) 3130, ν(C=O) 1647, ν(C=N) 1595, ν(N-N) 1020. ^1H NMR (δ, ppm (DMSO-d_6): 11.985 (s, 1H, NH), 9.516 (s, 1H, =CH), 8.759 (1H, Ar-H), 8.561 (1H, Ar-H), 8.316 (4H, Ar-H), 8.217 (1H, Ar-H), 8.188 (1H, Ar-H), 8.087 (1H, Ar-H), 7.975 (1H, Ar-H), 7.337 (1H, Ar-H), 6.724 (1H, Ar-H). ^{13}C NMR (δ, ppm (DMSO-d_6): 154.717 (C=O), 147.160 (HC=N), 146.482, 132.512, 131.435, 130.716, 129.319, 129.253, 128.973, 127.962, 127.483, 127.177, 126.672, 126.339, 125.820, 125.408, 124.716, 124.357, 122.893, 115.656, 112.755 (aromatic carbons).

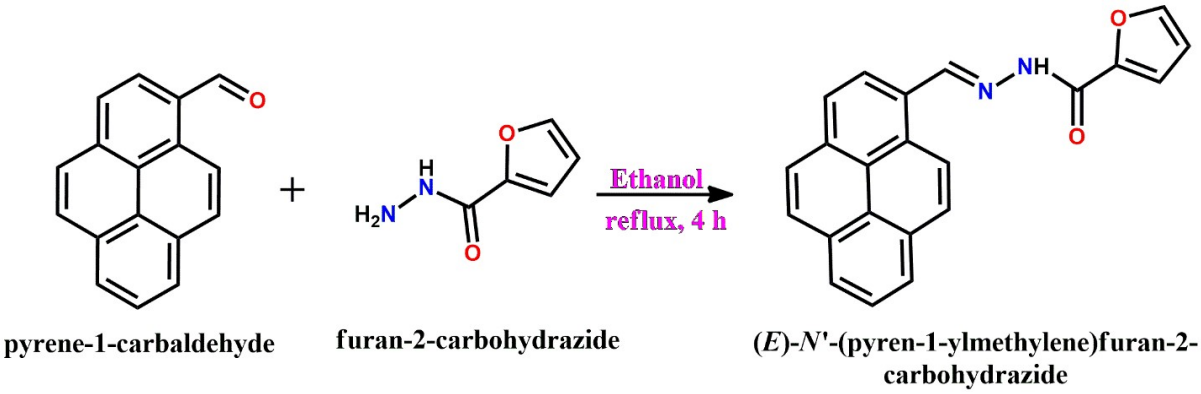

pyrene-1-carbaldehyde **furan-2-carbohydrazide** **(*E*)-*N*'-(pyren-1-ylmethylene)furan-2-carbohydrazide**

Scheme S1 Synthesis of PCFH

3. General procedures

Stock solution of PCFH (10 mM) has been prepared in DMF at room temperature. The concentration of PCFH was kept at 20 µM for all the experiments in solution state. 6 µL of PCFH was added with the help of microliter pipette to 3 mL of solvents for maintaining the desired concentrations. After each aliquot addition, the solution was uniformly mixed before recording the spectra. Aggregation-induced emission (AIE) properties were studied at 20 µM concentration of PCFH in THF/H_2O binary mixture with varying water content from 0 % to 99 % (f_w). Excitation wavelength of 350 nm and 405 nm have been optimized for photoluminescence spectroscopy in AIE and mechanochromic experiments, respectively.

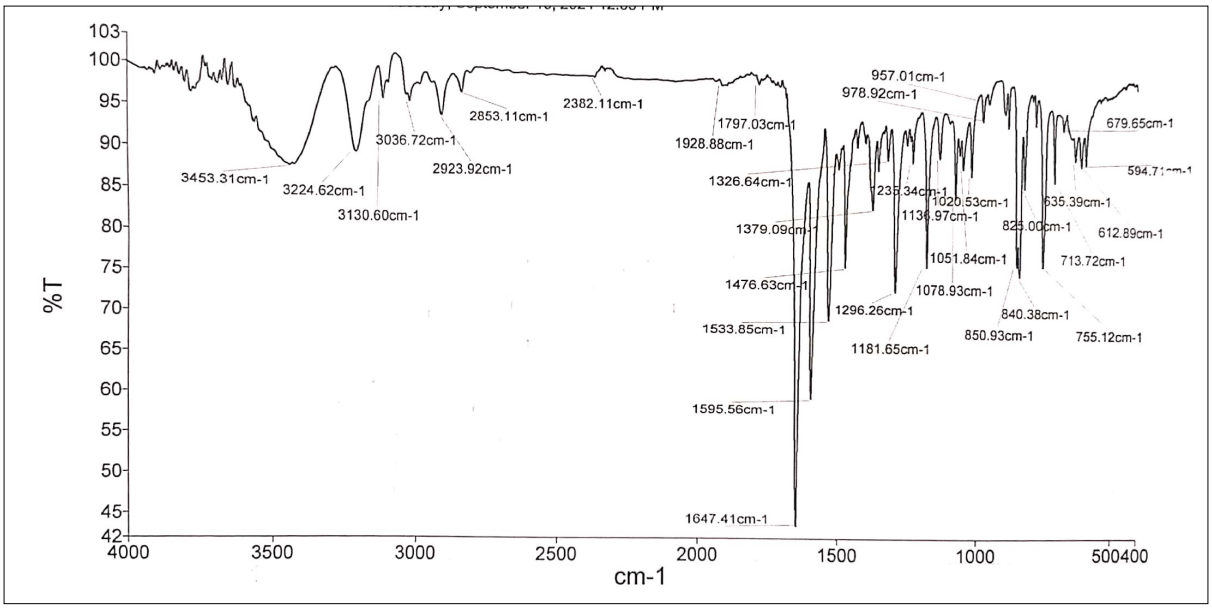

Fig. S1 IR spectrum of PCFH

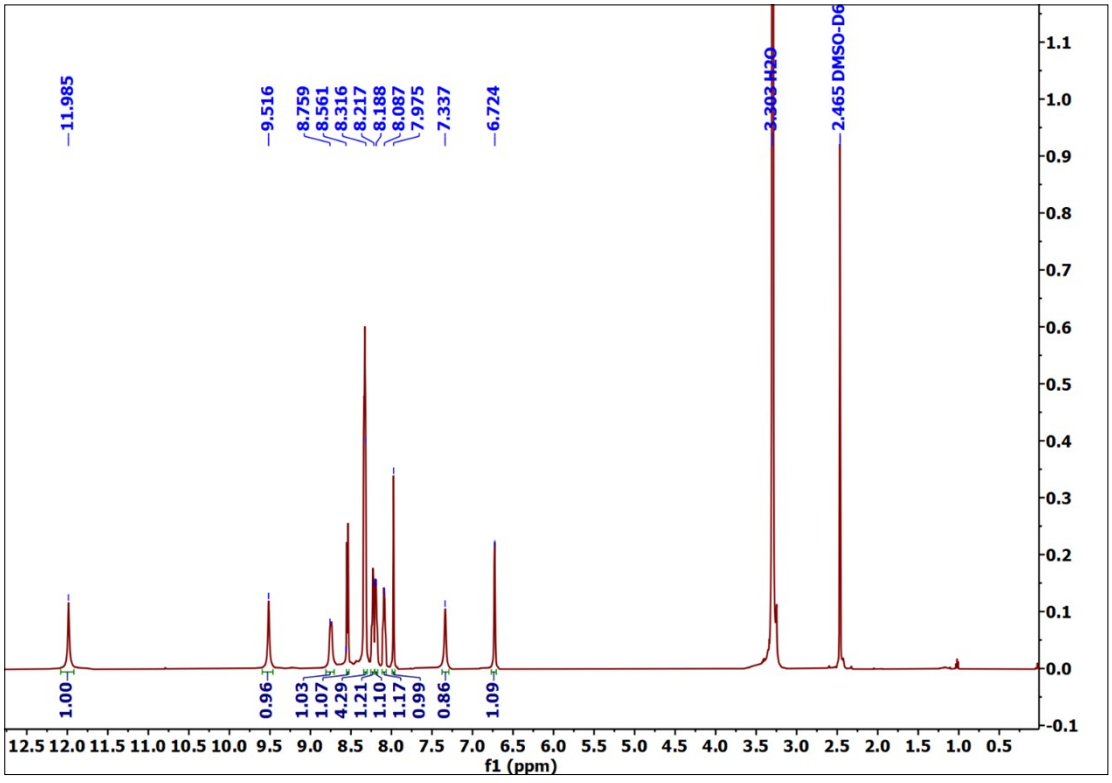

Fig.S2 ^{1}H NMR spectrum of PCFH in DMSO-d_6

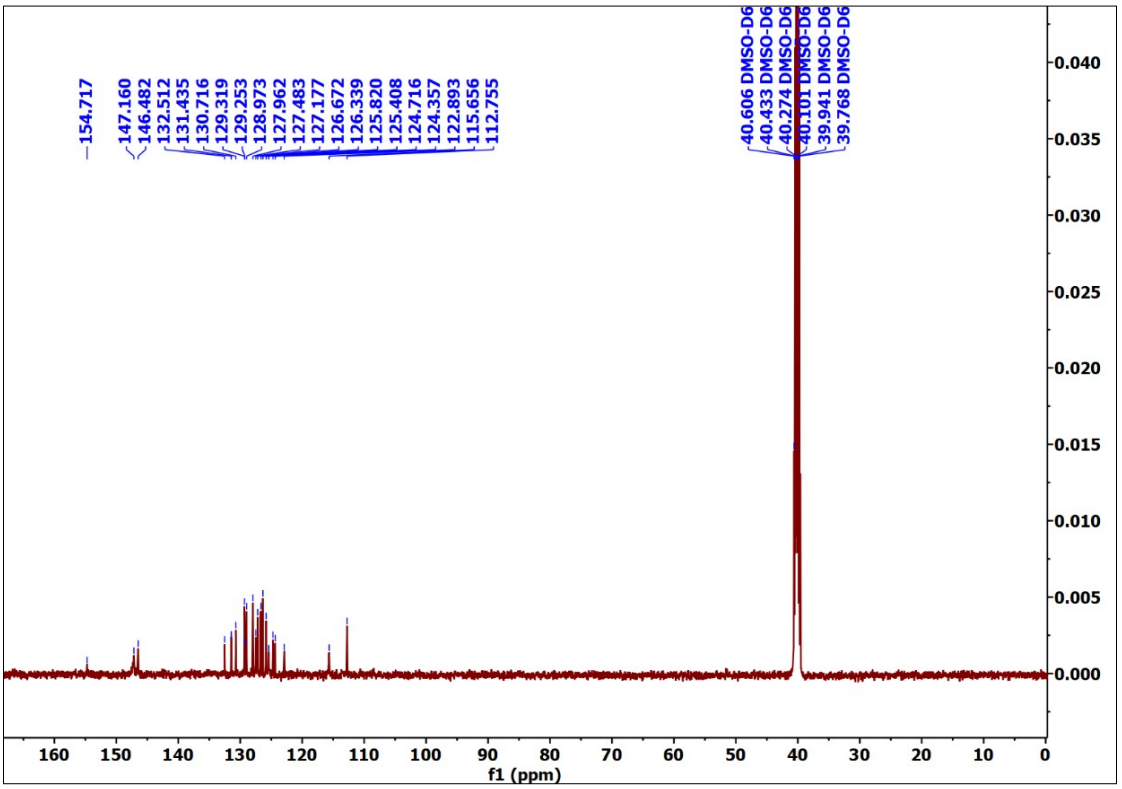

Fig.S3 ^{13}C NMR spectrum of PCFH in DMSO-d_6

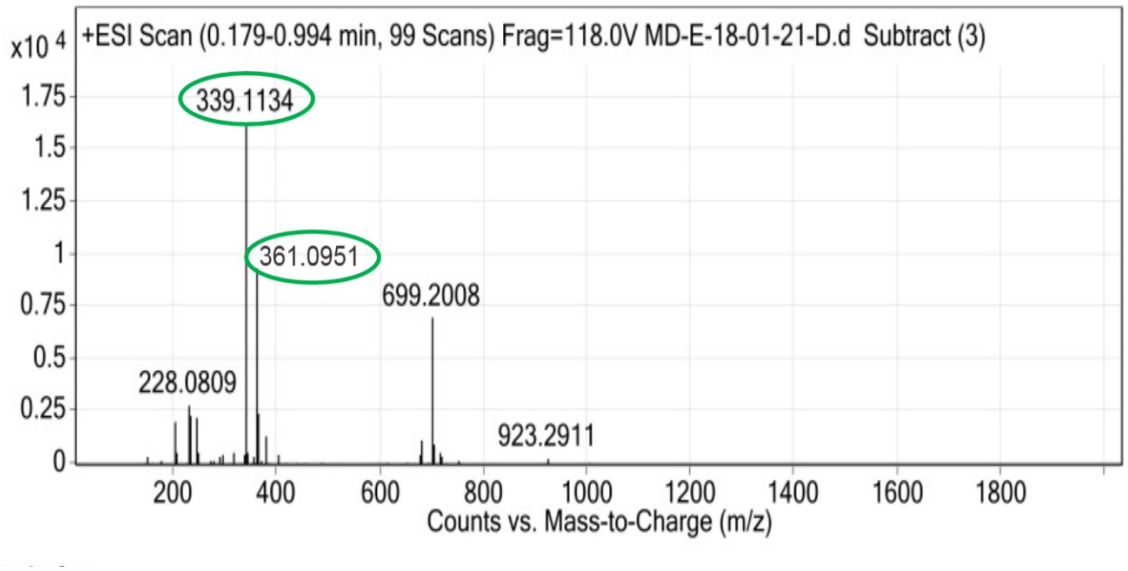

Fig. S4 High resolution mass spectrum of PCFH.

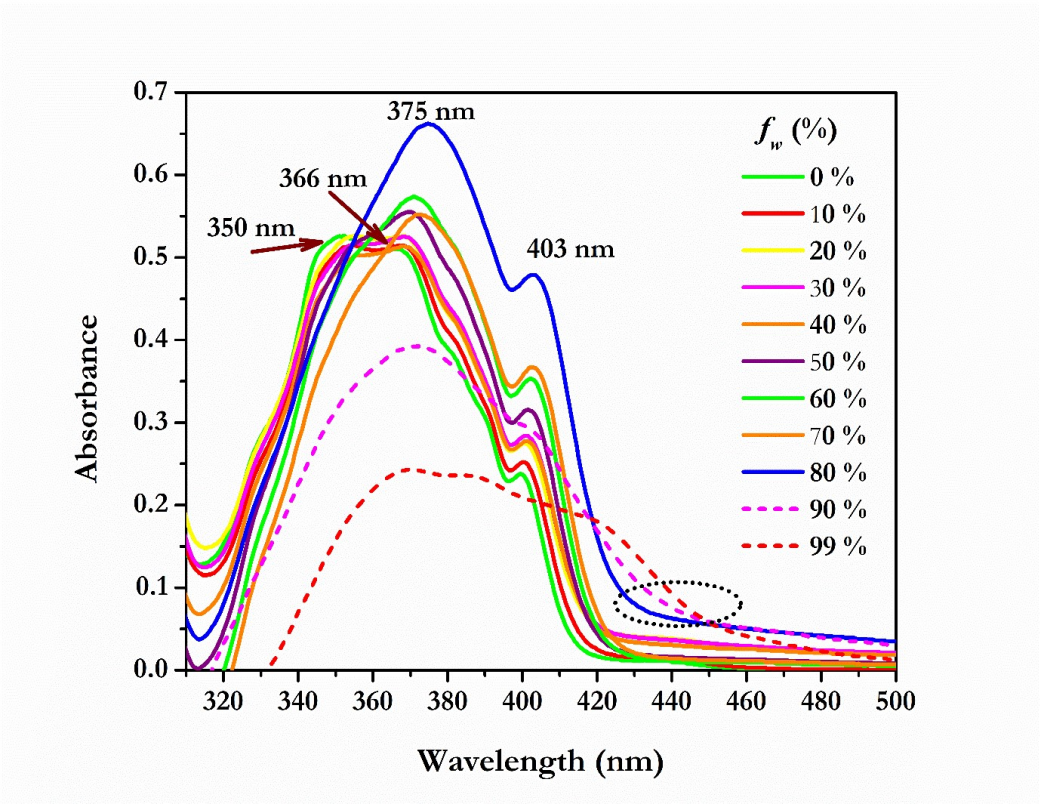

Fig. S5 Absorbance spectra of PCFH (20 μM) at different water fraction (f_w) in THF/H_2O binary solvent

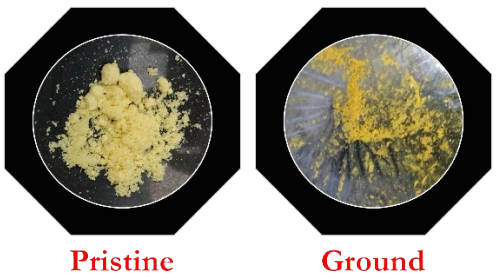

Fig. S6 Pristine and ground PCFH under visible light

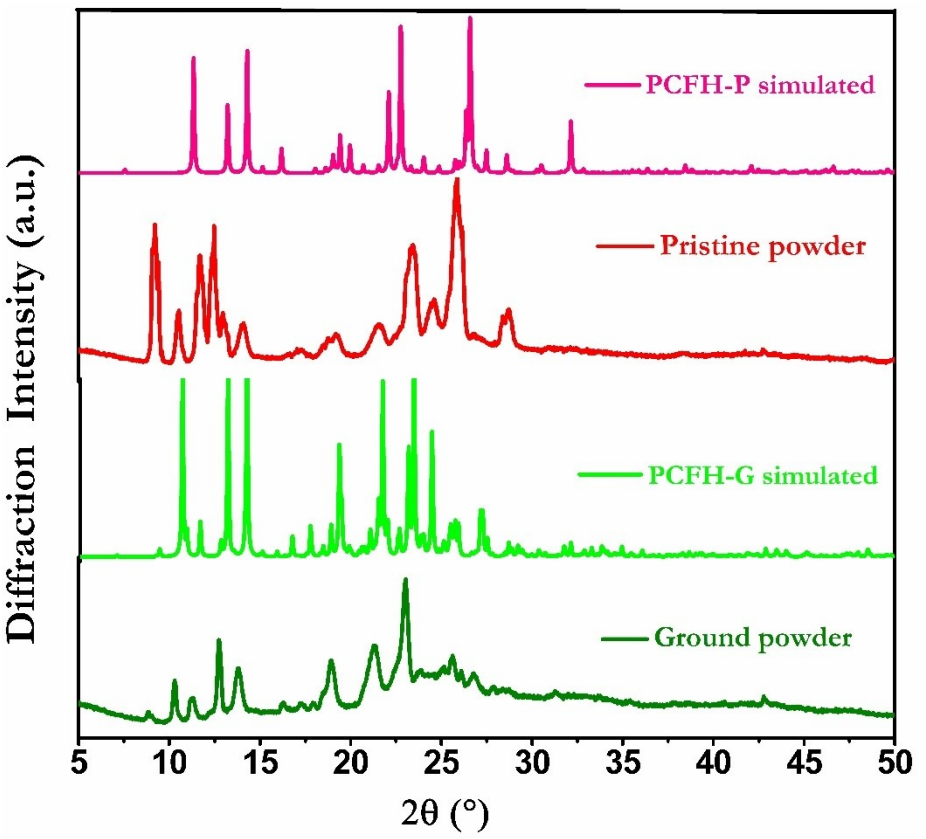

Fig. S7 PXRD patterns of Pristine and Ground powder compared with simulated patterns of PCFH-P and PCFH-G crystals

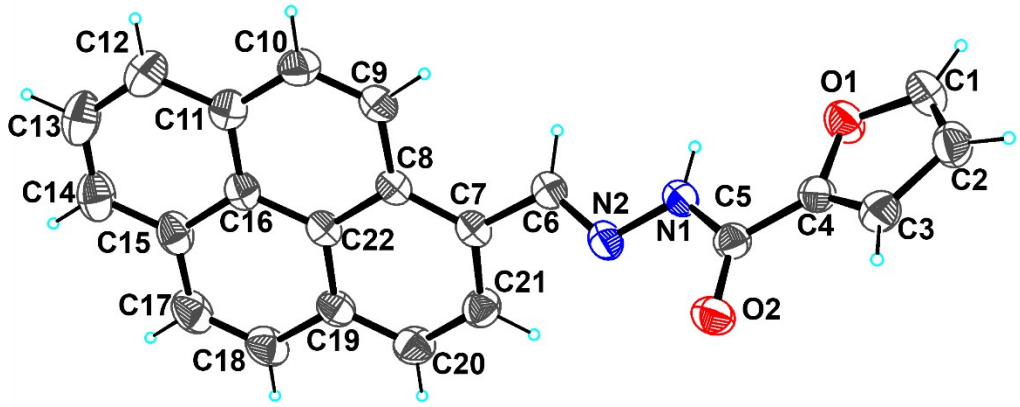

Fig. S8 ORTEP diagram of PCFH at 40% probability

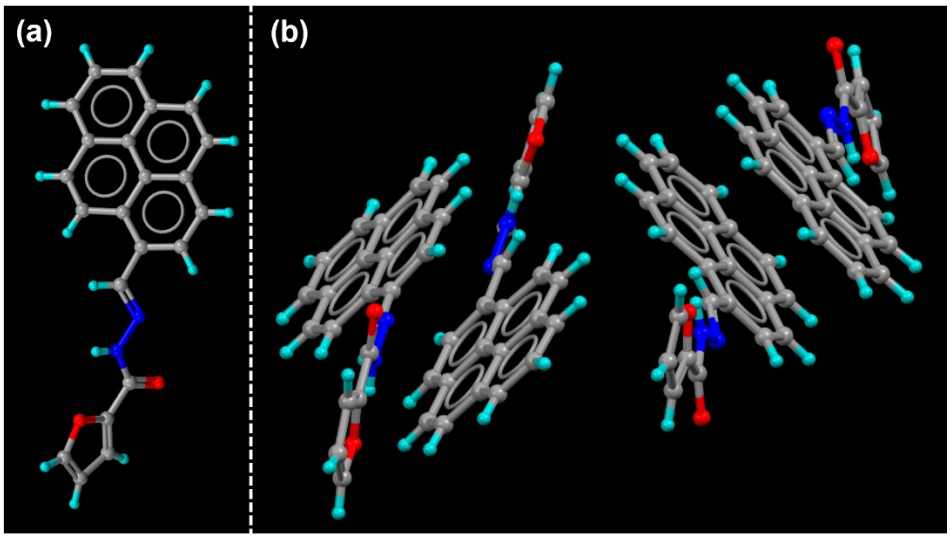

Fig. S9 Asymmetric units in PCFH-P and PCFH-G

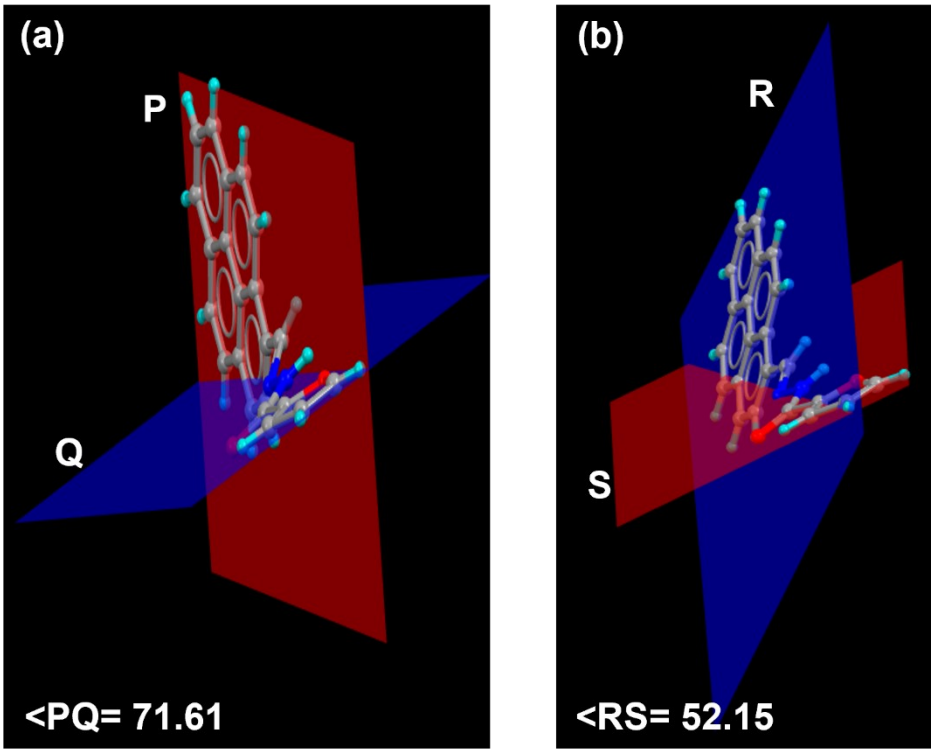

Fig. S10 Angle between least square mean plane of pyrene and furan ring in **(a)** PCFH-P and **(b)** PCFH-G crystals

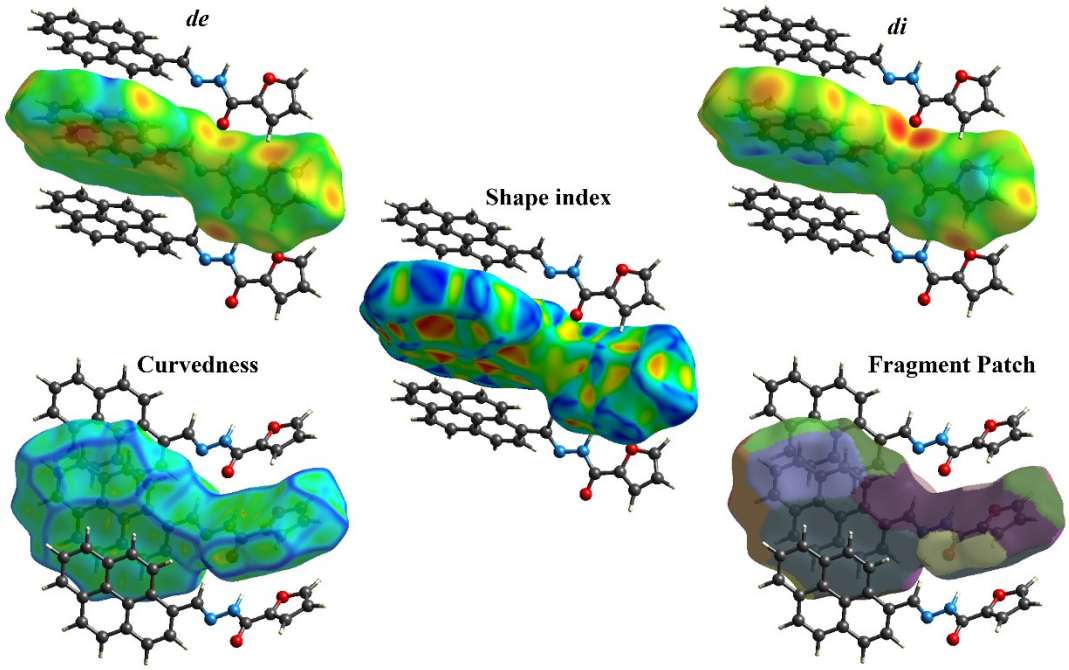

Fig. S11 Hirshfeld surfaces of PCFH-P polymorph

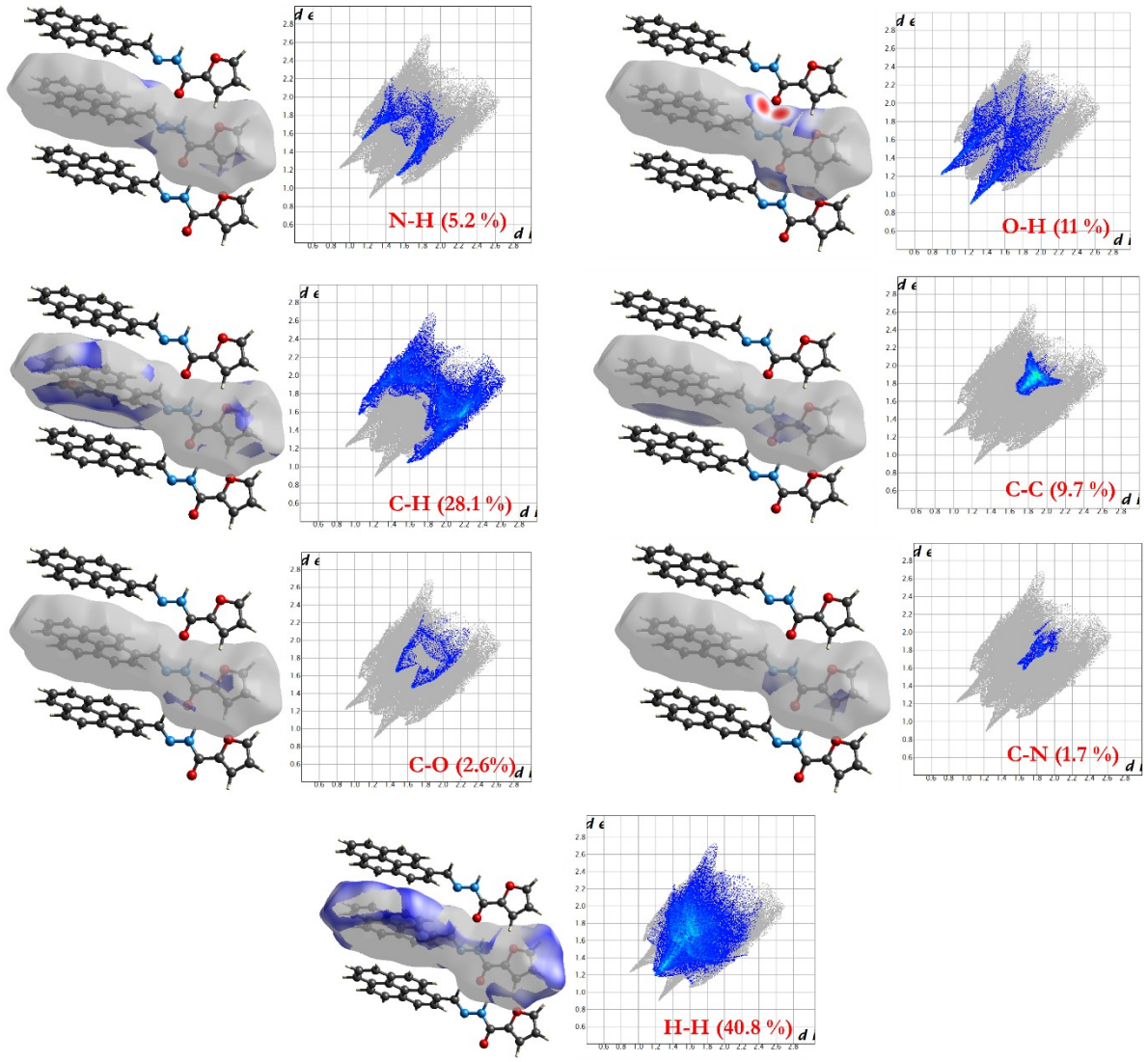

Fig. S12 Hirshfeld surfaces mapped over d_{norm} and 2D fingerprint plot demonstrating different intermolecular interactions in PCFH-P polymorph

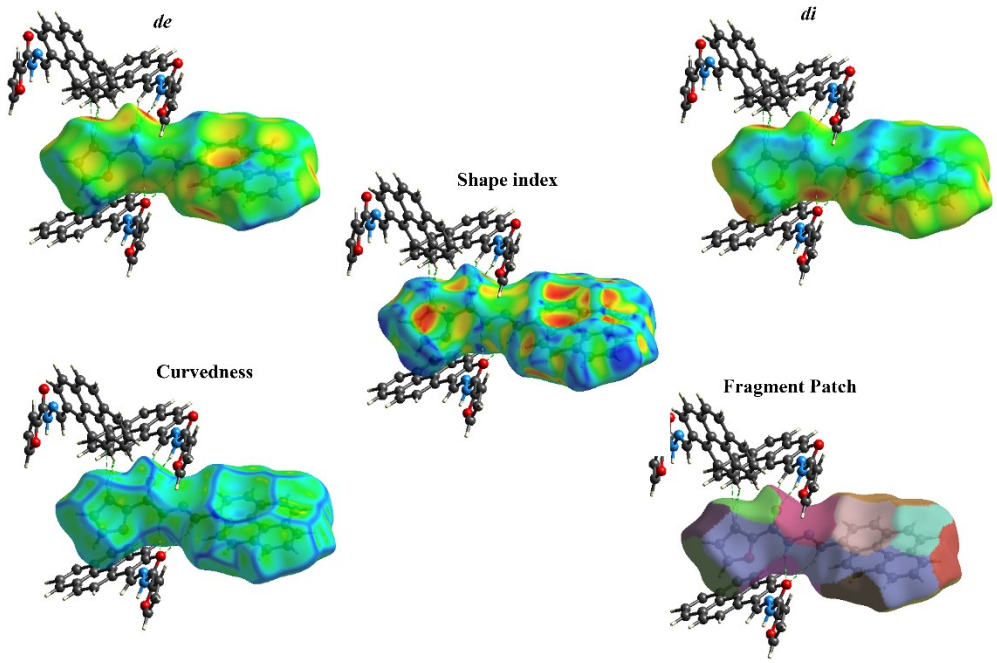

Fig. S13 Hirshfeld surfaces of PCFH-G polymorph.

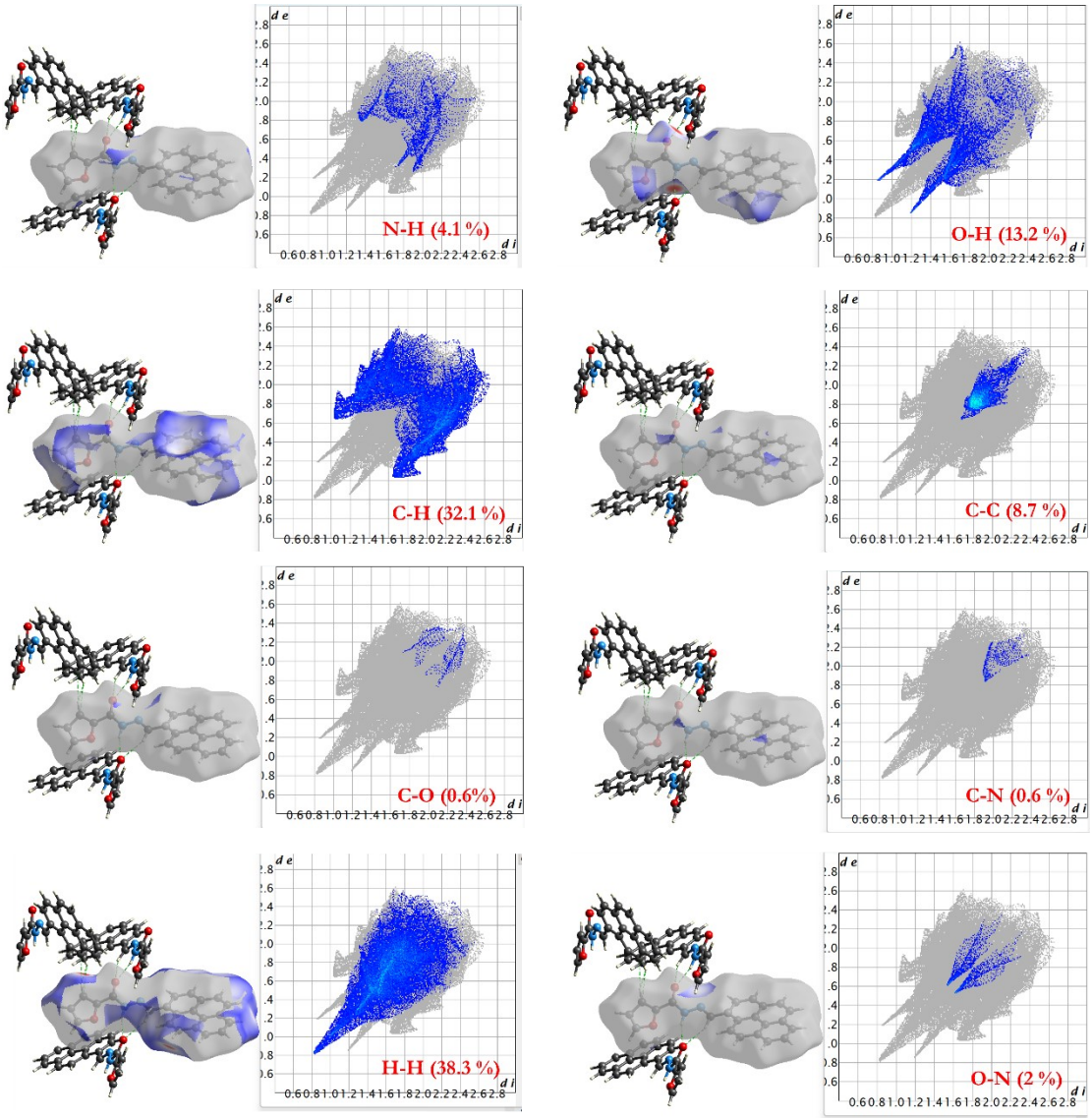

Fig. S14 Hirshfeld surfaces mapped over d_{norm} and 2D fingerprint plot demonstrating different intermolecular interactions in PCFH-G polymorph.

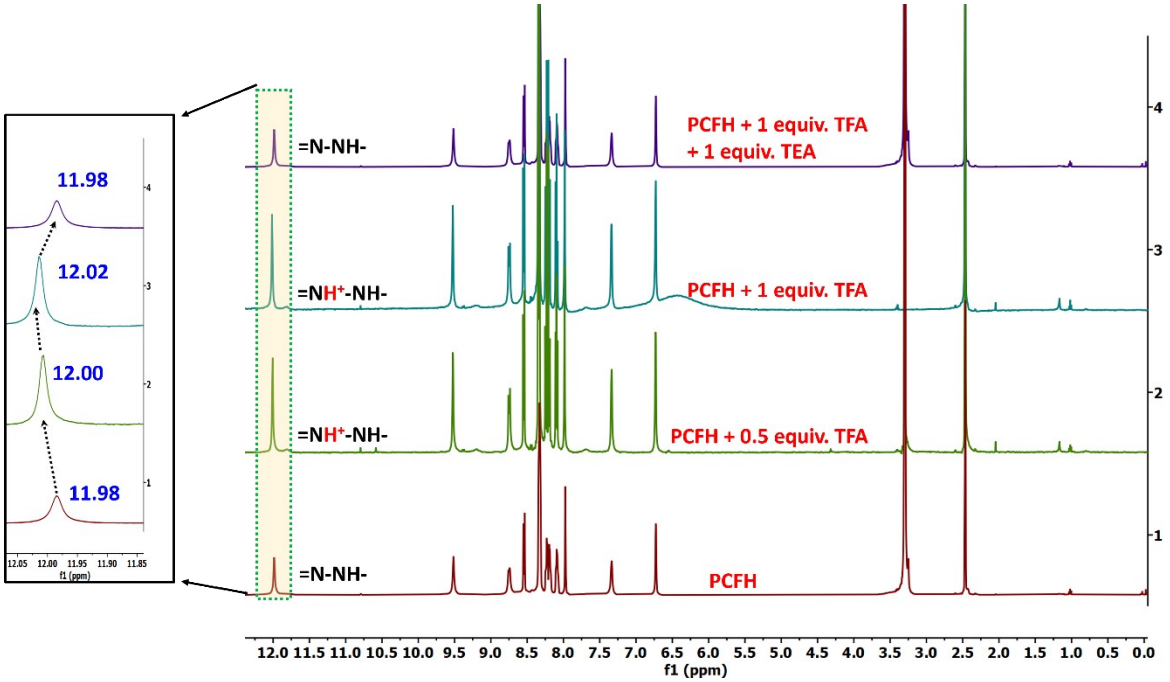

Fig. S15 ^{1}H NMR titration of PCFH upon sequential addition of TFA in DMSO-d_6.

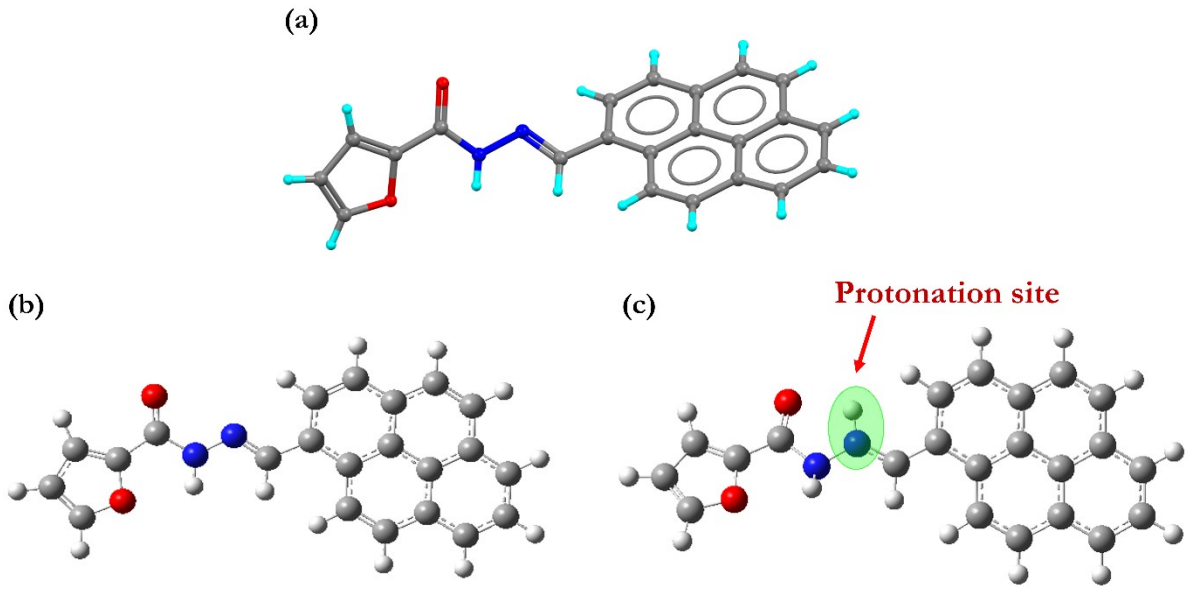

Fig. S16 (a) Ball-and-stick molecular structure of PCFH obtained from SC-XRD data. (b) DFT-optimized geometry of neutral PCFH, with the initial molecular structure generated from the CIF obtained from SC-XRD. (c) DFT-optimized geometry of protonated PCFH, generated by protonation of the DFT-optimized neutral PCFH; the protonation site is indicated by a green circle.

Table S1 Reported pyrene based mechanochromic materials

Molecular structure	Mechanochromic transformation	Crystal reported	Reference No.
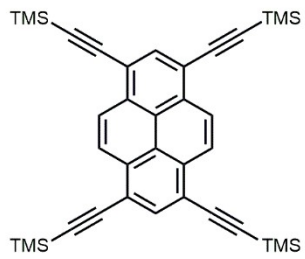	Crystalline → amorphous	No	50
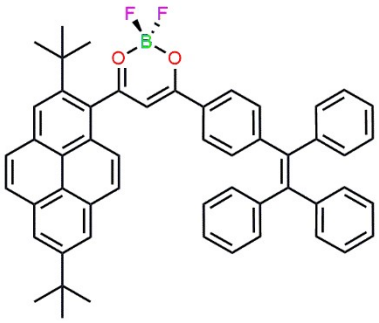	Crystalline → amorphous	No	51
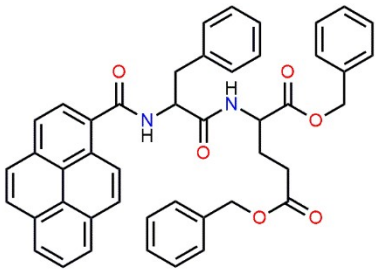	Ordered xerogel→ amorphous	No	52
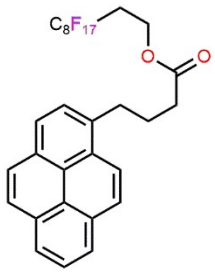	Crystalline → amorphous	No	53
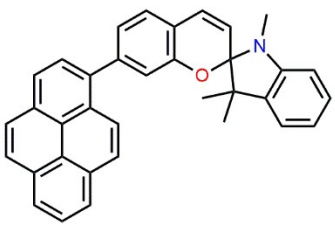	Crystalline → amorphous	No	34

	Crystalline → amorphous	No	54
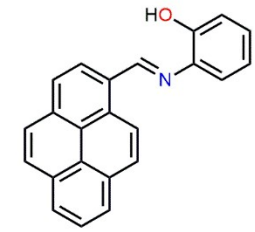	Crystalline → amorphous	No	55
	Crystalline → amorphous	No	56
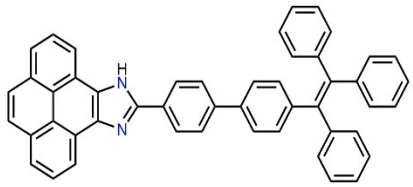	Crystalline → amorphous	No	57
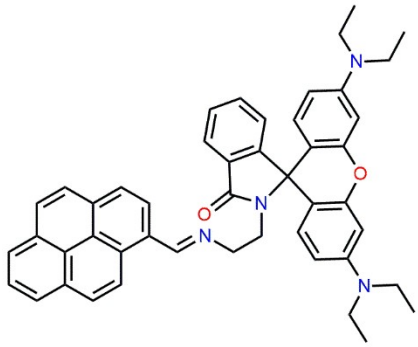	Crystalline → amorphous	No	33
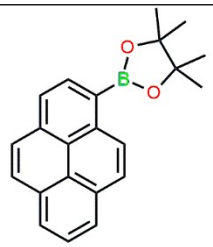	Crystalline → Semi crystalline	No	58

	Crystalline → Semi crystalline	No	59
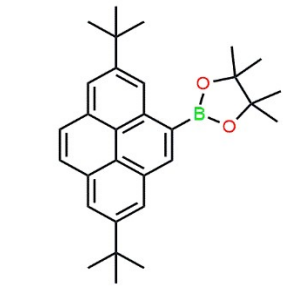	Crystalline → Semi crystalline	NO	60
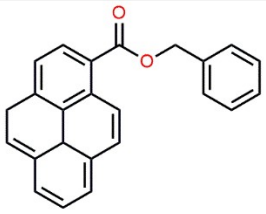	Crystalline → crystalline	No	31
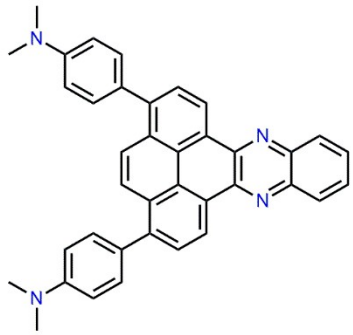	Crystalline → crystalline	Yes	14
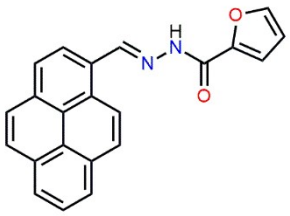	Crystalline → crystalline	Yes	This work

Table S2 Fluorescence decay parameters and quantum yield of PCFH in THF/H_2O mixtures at different fraction of water

f_w	<τ> (ns)	ϕ	K_r ($^{-}$s)	K_{nr} ($^{-}$s)
0 %	3.65	0.104	2.86 x 10^7	2.45 x 10^8
80 %	7.97	0.891	1.11 x 10^8	1.35 x 10^7
99 %	5.93	0.42	7.21 x 10^7	9.63 x 10^7

Table S3 Crystallographic data of PCFH-P and PCFH-G

Identification code	**PCFH-P**	**PCFH-G**
CCDC No.	2356829	2493464
Empirical formula	$C_{22}H_{14}N_2O_2$	$C_{88}H_{56}N_8O_8$
Formula weight	338.35	1353.40
Temperature/K	293(2)	293
Crystal system	monoclinic	orthorhombic
Space group	$P2_1/c$	Pnc2
a/Å	23.6495(6)	37.5695(5)
b/Å	5.02450(10)	19.2248(3)
c/Å	13.5103(3)	9.19900(10)
α/°	90	90
β/°	98.396(2)	90
γ/°	90	90
Volume/Å^3	1588.18(6)	6644.13(15)
Z	4	4
ρ_{calc}g/cm^3	1.415	1.353
μ/mm^{-1}	0.741	0.708
F(000)	704.0	2816.0
Crystal size/mm^3	0.2 × 0.1 × 0.05	0.11 × 0.09 × 0.06
Radiation	Cu Kα (λ = 1.54184)	Cu Kα (λ = 1.54184)
2Θ range for data collection/°	7.558 to 143.926	4.704 to 136.264
Index ranges	$-28 \le h \le 29$, $-6 \le k \le 4$, $-16 \le l \le 16$	$-45 \le h \le 38$, $-23 \le k \le 23$, $-11 \le l \le 11$
Reflections collected	9617	50913
Independent reflections	3061 [R_{int} = 0.0254, R_{sigma} = 0.0353]	11071 [R_{int} = 0.0677, R_{sigma} = 0.0431]
Data/restraints/parameters	3061/0/236	11071/1/938
Goodness-of-fit on F^2	1.018	1.039
Final R indexes [I>=2σ (I)]	R_1 = 0.0399, wR_2 = 0.1065	R_1 = 0.0720, wR_2 = 0.2146
Final R indexes [all data]	R_1 = 0.0541, wR_2 = 0.1150	R_1 = 0.0888, wR_2 = 0.2308
Largest diff. peak/hole / e Å^{-3}	0.20/-0.15	0.27/-0.21

Table S4 Selected bond length and bond angle of PCFH-P and PCFH-G

PCFH-P		**PCFH-G**	
Bond lengths (Å)			
O1-C4	1.368(17)	O1-C4	1.317(8)
O1-C1	1.363(19)	O1-C1	1.382(10)
O2-C5	1.228(17)	O2-C5	1.223(7)
N2-N1	1.385(17)	N2-N1	1.373(6)
N2-C6	1.278(2)	N2-C6	1.270(6)
N1-C5	1.351(19)	N1-C5	1.336(7)
C5-C4	1.461(2)	C5-C4	1.470(8)
Bond angles (°)			
C1-O1-C4	105.70(13)	C5-N1-N2	120.8(5)
C6-N2-N1	115.38(13)	C6-N2-N1	115.4(5)
C5-N1-N2	118.53(12)	C7-C8-C9	118.5(5)
O2-C5-N1	123.80(14)	N2-C6-C7	121.0(5)
O2-C5-C4	120.06(14)	C8-C7-C6	120.3(5)
N1-C5-C4	116.14(13)	N1-C5-C4	114.6(5)
C19-C22-C8	119.84(14)	O2-C5-N1	124.4(5)
C16-C22-C8	120.62(14)	C16-C11-C12	119.4(6)
C16-C22-C19	119.53(14)	C12-C11-C10	122.2(7)
C22-C8-C9	117.49(14)	O2-C5-C4	121.0(5)
C7-C8-C22	118.81(14)	C9-C10-C11	121.8(6)
C7-C8-C9	123.68(14)	O1-C4-C5	122.6(6)
C8-C7-C6	120.79(14)	C3-C4-C5	126.7(8)
C21-C7-C8	119.97(14)	C3-C4-O1	110.6(8)
C21-C7-C6	119.21(15)	C18-C17-C15	121.7(6)
O1-C4-C5	119.35(13)	C21-C19-C20	118.8(5)
C3-C4-O1	110.14(14)	C19-C20-C8	118.9(5)
C3-C4-C5	130.50(14)	C16-C20-C8	118.9(5)
C4-C3-C2	106.86(15)	C21-C19-C18	123.9(6)
C9-C10-C11	121.99(16)	C17-C15-C14	123.5(7)
C2-C1-O1	110.96(15)	C14-C15-C16	116.8(7)
C1-C2-C3	106.34(15)	C17-C15-C16	119.7(7)
		C4-O1-C1	121.9(6)
		C4-O1-C1	106.2(8)
		C2-C1-O1	108.9(10)
		C10-C9-C8	122.7(5)
		C4-C3-C2	105.3(10)